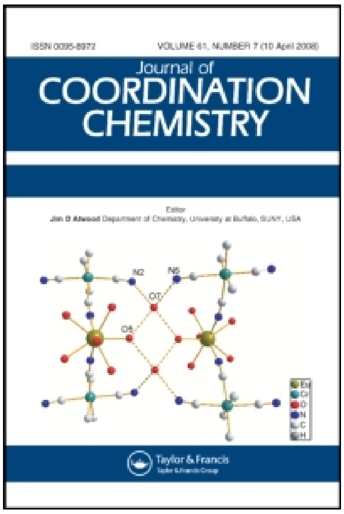

Journal of Coordination Chemistry
Publication details, including instructions for authors and subscription information:
http://www.informaworld.com/smpp/title~content=t713455674

A Zn(II)-Coordination Polymer Formed by Benzoate and 3-Pyridinemethanol Ligands: Synthesis, Spectroscopic Properties, Crystal Structure and Kinetics of Thermal Decomposition

V. Zeleák[a]; I. Císařová[b]; M. Sabo[a]; P. Llewellyn[c]; K. Gyoryová[a]
[a] Department of Inorganic Chemistry, Faculty of Natural Science, Institute of Chemical Sciences, P.J. Šafárik University, Moyzesova 11, SK-041 54 Košice, Slovakia [b] Department of Inorganic Chemistry, Charles University, Hlavova 2030, Prague, Czech Republic [c] Madirel Laboratory (UMR 6121), Provence University and CNRS, Centre de St-Jérôme, F-13331 Marseille, France

To cite this Article Zeleák, V. , Císařová, I. , Sabo, M. , Llewellyn, P. and Gyoryová, K.(2004) 'A Zn(II)-Coordination Polymer Formed by Benzoate and 3-Pyridinemethanol Ligands: Synthesis, Spectroscopic Properties, Crystal Structure and Kinetics of Thermal Decomposition', Journal of Coordination Chemistry, 57: 2, 87 — 96

To link to this Article: DOI: 10.1080/00958970410001662444

URL: http://dx.doi.org/10.1080/00958970410001662444

J. Coord. Chem., Vol. 57, No. 2, 20 January 2004, pp. 87–96

Taylor & Francis
Taylor & Francis Group

A Zn(II)-COORDINATION POLYMER FORMED BY BENZOATE AND 3-PYRIDINEMETHANOL LIGANDS: SYNTHESIS, SPECTROSCOPIC PROPERTIES, CRYSTAL STRUCTURE AND KINETICS OF THERMAL DECOMPOSITION

V. ZELEŇÁK[a,]*, I. CÍSAŘOVÁ[b], M. SABO[a],
P. LLEWELLYN[c] and K. GYORYOVÁ[a]

[a]*Department of Inorganic Chemistry, Faculty of Natural Science, Institute of Chemical Sciences, P.J. Šafárik University, Moyzesova 11, SK-041 54 Košice, Slovakia;* [b]*Department of Inorganic Chemistry, Charles University, Hlavova 2030, Prague, Czech Republic;* [c]*Madirel Laboratory (UMR 6121), Provence University and CNRS, Centre de St-Jérôme, F-13331 Marseille, France*

(Received in final form 20 October 2003)

The complex *catena*-poly[bis(benzoato-*O*)-bis(3-pyridinemethanol-*N*,*O*)-zinc(II)], $[Zn(benz)_2(3\text{-pymeth})_2]_n$ was prepared and characterised by elemental analysis, IR spectroscopy, thermal analysis and an X-ray structure determination. Zinc is octahedrally coordinated. Two coordination sites are occupied by oxygen atoms of two monodentate benzoate groups, two by the nitrogen atoms of 3-pyridinemethanol, and two by methanolic oxygen atoms of 3-pyridinemethanol from neighbouring structural units. Due to the bridging 3-pyridinemethanol ligand, molecules of the complex are connected into infinite chains along the *c* axis. The bridging function is reflected in the IR spectrum by a very sharp absorption band due to the stretching vibration of the methanolic O–H group. Non-isothermal kinetics of the thermal decomposition were studied using the model-free isoconversional method. Based on isoconversional dependencies, a multi-step mechanism with parallel reactions was recognised for the decomposition of the complex.

Keywords: Zinc benzoate; 3-Pyridinemethanol; Crystal structure; FT-IR; Thermogravimetry; Model-free kinetics

INTRODUCTION

Zinc is an essential and beneficial element in human growth. It is the second most abundant transition metal in the human organism following iron. This element is known to regulate activity in over 300 metalloenzymes and as a component of "zinc fingers" participates in the reliable transfer of genetic information [1–3].

In addition to physiological functions, zinc and its compounds have important roles in clinical medicine. Antibacterial and antiviral activity and the wound-healing effect

---

*Corresponding author. E-mail: zelenak@kosice.upjs.sk

ISSN 0095-8972 print: ISSN 1029-0389 online
DOI: 10.1080/00958970410001662444

of zinc-containing ointments has been known for several centuries [4–9]. Zinc may be used as a therapeutic agent and it may act as an antisickling agent and play a role in the prevention of pain crises in sickle-cell disease. Zinc has been successfully used in the treatment of acrodermatitis enteropathica, Wilson's disease, gastrointestinal disorders, infertility and other diseases [10].

In addition to conventional zinc compounds (zinc sulfate, zinc oxide), complexes with organic ligands are also often used in clinical medicine and cosmetics. The complex of zinc (II) with pyrithione is used in shampoos as an anti-dandruff agent [11]. The complex of zinc (II) acetate with erythromycin is used for acne therapy [12,13]. It is still of interest to find new compounds with enhanced activity against various strains of bacteria. In this task it is important to study synergetic or antagonistic effect between zinc and the molecules which themselves have antibacterial properties, e.g., benzoic acid. Benzoic acid is used in combination with salicylic acid in dermatology as a fungicidal treatment (Whitfield's ointment) for fungal skin diseases (ringworm) [14]. It can be found in cosmetics, deodorants and toothpaste [15,16]. More widespread is the use of benzoic acid and its salts to preserve food from growth of micro-organisms and it can be found in beverages, fruit products, chemically leavened baked goods and condiments, and is used in the beverage industry (E-codes 210-213) [17–21].

As a part of our continuing research concerning properties, crystal structures and biological activity of zinc(II) complexes with carboxylic acids we have described properties of two molecular zinc(II) benzoate complexes with the pyridine-based ligands nicotinamide and methyl-3-pyridylcarbamate [22]. The present article is an extension of our research and describes the properties of the polymeric complex *catena*-poly[bis-(benzoato-*O*)-bis(3-pyridinemethanol-*N*,*O*)-zinc(II)], [Zn(benz)$_2$(3-pymeth)$_2$]$_n$. The biological activity of these complexes against common strains of bacteria is under investigation.

EXPERIMENTAL

Synthesis

Some 25 cm^3 of an aqueous solution of sodium benzoate (0.500 g, 3.47 mmol) was mixed with 25 cm^3 of an aqueous solution of zinc sulfate (0.280 g, 1.73 mmol). The pH of the solution was adjusted to 6 using free benzoic acid. After 30 min stirring, the solution was filtered and 3-pyridinemethanol (0.378 g, 3.47 mmol) was added to the filtrate. The reaction mixture was stirred for 3 h then filtered and left to stand at room temperature. After two days colourless prisms crystallised. The crystals were filtered off, washed with water and dried. Yield 79%. Anal, Calcd. for $C_{26}H_{24}N_2O_2Zn$ (%): C, 59.38; H, 4.60; N, 5.33; Zn, 12.43. Found: C, 59.12; H, 4.23; N, 5.45; Zn, 12.78. IR (KBr disc): 3436m, 3057w, 2932w, 2866w, 1618vs, 1607vs, 1552vs, 1482w, 1437 s, 1392vs, 1351s, 1313m, 1249m, 1216m, 1197m, 1177w, 1113m, 1059s, 1033w, 993vw, 951vw, 926w, 824s, 794m, 718vs, 703s, 650s, 618w, 557w, 454m, 414w, cm^{-1}.

Physical Measurements

The infrared spectrum of the complex was recorded with an EQUINOX 55 (Bruker) FT-IR spectrophotometer using KBr discs (complex/KBr mass ratio 1 : 100).

Thermogravimetric (TG) measurements were carried out in a static air atmosphere with a heating rate of 5, 10 and 20°C min^{-1} using a Derivatograph MOM apparatus. The sample size was 50 mg. Elemental analysis (C, H, N) was performed with a Perkin-Elmer 2400 CHN instrument. Zinc was determined spectrophotometrically by the dithizone method with a Varian 635 spectrophotometer.

Structure Determination and Refinement

The complex crystallised as air-stable, colourless prisms. Diffraction experiments were performed at 150 K with a Nonius-Kappa CCD diffractometer (Mo Kα radiation, $\lambda = 0.71070$ Å) equipped with a graphite monochromator and a low-temperature goniometer. Unit cell parameters were determined by a least-squares fit to 7627 reflections (θ from 1 to 27.5°). Details of the data collection are summarised in Table I. Data were corrected for Lorentz and polarisation factors. Zinc was located from a

TABLE I Crystal data and structure refinement details

Empirical formula	$C_{26}H_{24}N_2O_6Zn$
Formula weight	525.84
Crystal parameters	
Crystal shape	Prisms
Crystal colour	White
Crystal size (mm)	0.37 × 0.32 × 0.3
Crystal system	Monoclinic
Space group	*C*2/*c* (No. 15)
Unit-cell dimensions	
a(Å)	17.7530(4)
b(Å)	11.3440(2)
c(Å)	13.0920(3)
β (°)	118.794(1)
V(Å^{-3})	2310.60(8)
Molecules per cell, Z	4
D_x (g cm^{-3})	1.512
Measurement of intensity data	
Instrument	Nonius Kappa CCD
Temperature (K)	150(2)
Radiation λ (Å)	0.71070
Monochromator	Graphite
Scan mode	φ and ω
θ range (°)	3.21–27.49
Reflections measured	15 385
Independent reflections	2617
Reflections observed	2304 ($I \geq 2\sigma(I)$)
Linear absorption coefficient μ (mm^{-1})	1.109
F(000)	1088
Reflections for cell measurement	7627
Indices limits	
h	−23 to 23
k	−14 to 14
l	−16 to 17
Refinement method	Full-matrix least-squares on F^2
Parameters	208
Goodness-of-fit on F^2	1.0110
R_1	0.0270 (observed); 0.0320 (all)
wR_2	0.0801 (observed); 0.0841 (all)
Max./min. height in final difference synthesis (e Å^{-3})	0.302/− 0.462

TABLE II Selected bond distances (Å) and angles (°) in the complex $[\mathrm{Zn(benz)_2(3\text{-}pymeth)_2}]_n$

Bond distances			
Zn–O(2)	2.046(1)	O(1)–C(1)	1.251(2)
Zn–N(1)	2.141(1)	O(2)–C(1)	1.268(2)
Zn–O(3)	2.204(1)	O(3)–C(13)	1.423(2)
N(1)–C(12)	1.342(2)	C(1)–C(2)	1.508(2)
N(1)–C(8)	1.347(2)		
Bond angles			
O(2)–Zn–O(2)	174.62(5)	O(2)–Zn–O(3)$^{\mathrm{iii}}$	87.93(4)
O(2)–Zn–N(1)$^{\mathrm{i}}$	93.71(4)	N(1)–Zn–O(3)$^{\mathrm{iii}}$	176.86(3)
O(2)–Zn–N(1)	89.95(4)	O(3)$^{\mathrm{ii}}$–Zn–O(3)$^{\mathrm{iii}}$	89.63(5)
N(1)–Zn–N(1)$^{\mathrm{i}}$	94.47(6)	O(1)–C(1)–O(2)	125.4(1)
O(2)–Zn–O(3)$^{\mathrm{ii}}$	88.25(4)	O(1)–C(1)–C(2)	118.6(1)
O(2)$^{\mathrm{i}}$–Zn–O(3)$^{\mathrm{ii}}$	87.94(4)	O(2)–C(1)–C(2)	116.0(1)
N(1)$^{\mathrm{i}}$–Zn–O(3)$^{\mathrm{ii}}$	176.86(3)	O(3)–C(13)–C(9)	110.9(1)
N(1)–Zn–O(3)$^{\mathrm{ii}}$	87.99(5)		

i = $-x$, y, $-z+0.5$; ii = $-x$, $1-y$, $-z$; iii = x, $1-y$, $0.5+z$.

Patterson synthesis using SHELXS97 [23]. Fourier maps, calculated using SHELXL97 [24], allowed the location of all non-hydrogen atoms. Full-matrix least-squares refinements on F^2 were carried out with anisotropic thermal parameters for non-hydrogen atoms. Hydrogen atoms were located from a difference Fourier synthesis and refined isotropically. Final reliability values are summarised in Table I while selected bond distances and angles are listed in Table II. Figures were prepared using DIAMOND [25] software.

RESULTS AND DISCUSSION

Description of the Structure

A view of the structure of the complex $[\mathrm{Zn(benz)_2(3\text{-}pymeth)_2}]_n$ is shown in Fig. 1. The complex crystallises in the monoclinic space group $C2/c$ with four formula units in the unit cell. Zinc is octahedrally coordinated and lies in a special position on a crystallographic two-fold axis. Two coordination sites are occupied by oxygen atoms of monodentate benzoate groups, two by the nitrogen atoms of the pyridine ring of 3-pyridinemethanol and two by the methanolic oxygen atoms of pyridinemethanol ligands from neighbouring structural units (see Fig. 1). The bridging function of 3-pyridinemethanol allows the molecules of the complex to form infinite chains running along the *c* axis (Fig. 2). This bridging function was also observed in copper(II) complexes [26,27]. However, in contrast to the Cu(II) complexes, whose oxygen atoms of 3-pyridinemethanol ligands occupy positions opposite each other in the octahedron (*trans*), in the studied zinc(II) complex the oxygen atoms lie in *cis* positions. In addition to bidentate coordination of the 3-pyridinemethanol described above, only monodentate coordination of this ligand was found in the complex tetrakis-μ-acetato-bis(3-pyridinemethanol)dicopper(II) [28].

The distances of the coordinated benzoate oxygen atoms from zinc are 2.046(1) Å, in the range of values observed for octahedral zinc benzoate complexes with monodentate carboxylate coordination [29–31], and are longer than values observed for tetrahedral

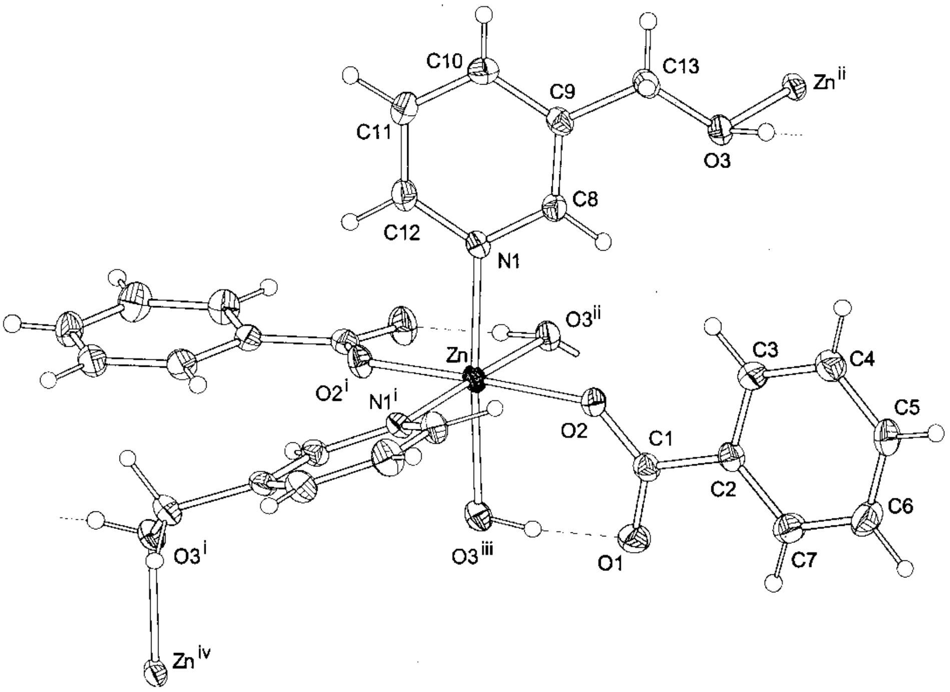

FIGURE 1 The structure of the complex $[Zn(benz)_2(3\text{-pymeth})_2]_n$ with the atom labelling scheme. Symmetry codes: (i) $-x, y, -z+0.5$; (ii) $-x, 1-y, -z$; (iii) $x, 1-y, 0.5+z$; (iv) $-x, 1-y, 1-z$.

complexes [32–37]. Uncoordinated carboxylate oxygen in complexes is often involved in a weak interaction with the metal ion, leading to distortion of the coordination polyhedron [38]. However, in the studied complex this distance is too long [3.419(2) Å] for effective interaction and the angles in the zinc polyhedron differ only slightly from the ideal 90° value (see Table II).

Uncoordinated carboxylate oxygen atom O(1) and the hydrogen atom of a methanolic group H(12), are linked by a hydrogen bond [$O(3)\text{–}H(12)\cdots O(1)^i = 1.69(3)$ Å; $O(3)\text{–}H(12)\cdots O(1)^i = 168(3)°$; $i = -x, y, 1/2 - z$; see dashed lines in Fig. 1]. No other intramolecular or intermolecular hydrogen bonds, which would increase the dimensionality of the system, were found.

Spectroscopic Studies

IR data for the complex are listed in the Experimental Section. Solid state FT-IR spectra of the complex show the presence of coordinated benzoate and 3-pyridinemethanol ligands. The stretching vibration of the methoxy group of pyridinemethanol was found at $3436\,cm^{-1}$. In comparison to the free, uncoordinated 3-pyridinemethanol molecule where this band is broad, in the complex it is intense and sharp. Similar intense and sharp bands for the stretching vibration of the –OH group were observed in complexes with bridging hydroxo groups [31]. Aromatic and aliphatic C–H stretching vibrations are observed at 3057, 2932 and $2866\,cm^{-1}$.

In the IR spectra of carboxylates the stretching vibrations of the carboxylate group $\nu_{as}(COO)$ and $\nu_s(COO)$ are characteristic. In the complex these bands are

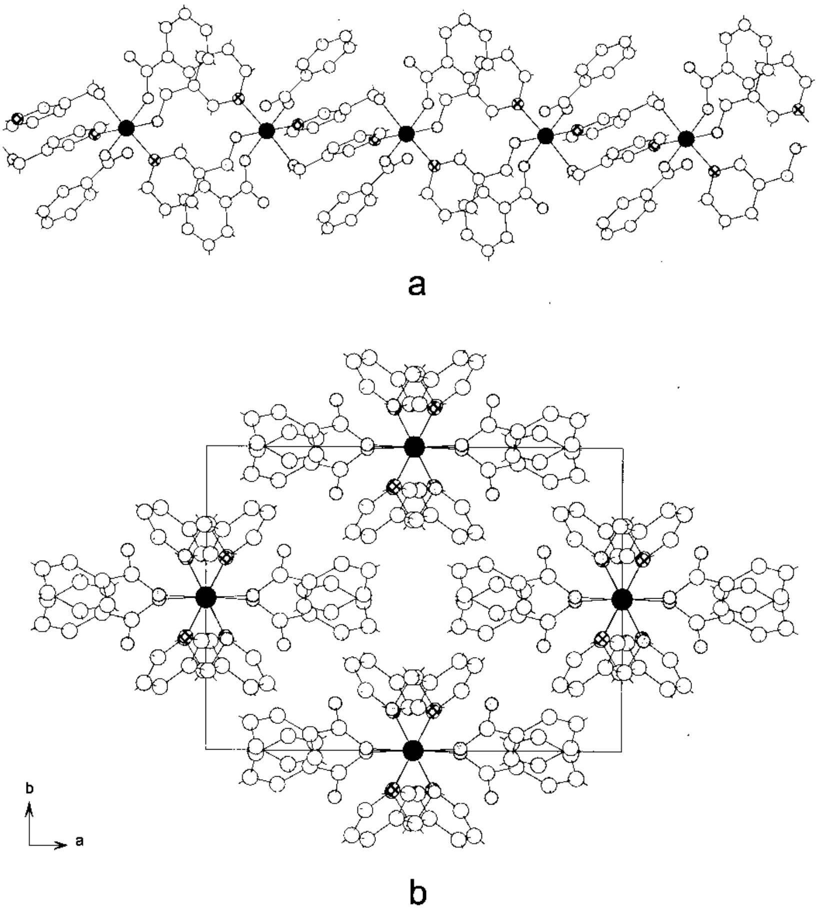

FIGURE 2 (a) View of one of the 1D chains running along crystallographic *c* axis; (b) view along the *c* axis showing the packing of the chains. Zinc atoms are displayed as black spheres, oxygen atoms as grey spheres, nitrogen atoms as hatched spheres and carbon atoms as white spheres. Hydrogen atoms are omitted for clarity.

at 1618 and 1392 cm^{-1}, respectively. The high separation of the bands $\Delta = \nu_{as}(COO) - \nu_s(COO) = 226\,cm^{-1}$ is consistent with monodentate carboxylate coordination [39,40]. In the region between 1600 and 1400 cm^{-1} and below 1300 cm^{-1} a number of bands due to stretching vibrations of aromatic rings as well as deformation vibrations of C–H bonds and the aromatic ring are observed and values are listed in the Experimental Section.

Structure and Thermal Stability Correlation

Phenomenological Aspects

Thermal analysis curves (TG/DTG) of the complex $[Zn(benz)_2(3\text{-pymeth})_2]_n$ are presented in Fig. 3. The two-step decomposition process is consistent with the crystal structure of the complex described above, where two pairs of the same ligand (3-pyridinemethanol or benzoate), are related through a crystallographic

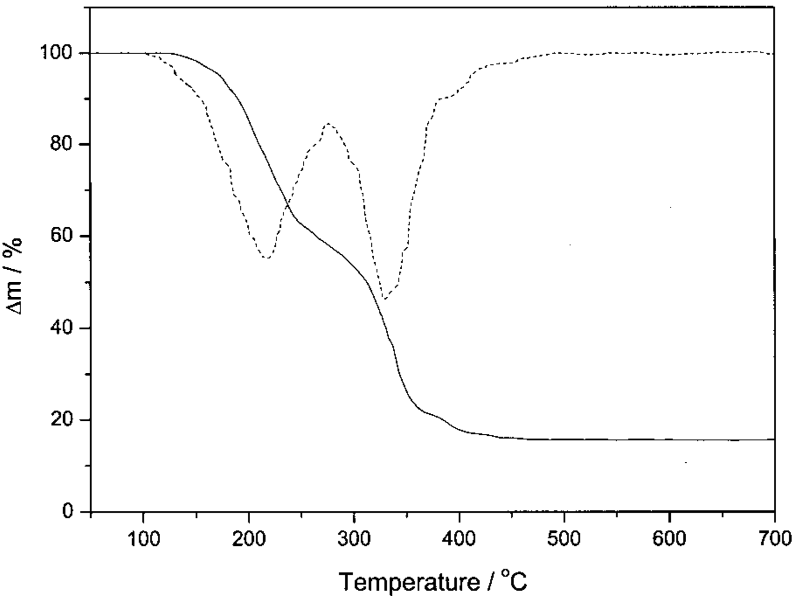

FIGURE 3 Experimental TG (solid line) and DTG (dashed line) curves of the complex $[Zn(benz)_2(3\text{-pymeth})_2]_n$ obtained during heating in air at 10 K min^{-1}.

two-fold axis. The first step in the thermal decomposition in the range 120–280°C was accompanied by a weight loss of 42%. In the next step, in the range 280–480°C, a weight loss of 43% was observed. In the final solid residue (15% of the initial mass), zinc oxide was detected by X-ray powder diffraction [41].

From the observed weight losses in the first and second steps of the thermal decomposition it was not possible to distinguish unmistakably, which ligand (3-pyridinemethanol or benzoate) was liberated, respectively. The calculated weight loss is similar for both ligands (41.5 and 43%). However, considering the higher volatility of the 3-pyridinemethanol (b.p. ~137–140°C) and literature data [42], we suggest that in the first step 3-pyridinemethanol ligands are liberated while in the second step pyrolysis of benzoate takes place.

Kinetic Aspects

To study the non-isothermal kinetics the isoconversional (model-free) Ozawa–Flynn–Wall method was used [43,44]. Isoconversional methods were recommended for kinetic studies by the ICTAC kinetic project [45,46]. Before evaluation of the kinetics, the experimental TG curves, obtained at heating rates 5, 10 and 20 K min^{-1} were transformed into degree of conversion data according to Eq. (1),

$$\alpha(t) = \frac{\%m_s - \%m_t}{\%m_s - \%m_f} \tag{1}$$

where $\%m_s$ is the initial percentage mass, $\%m_t$ is the percent mass at time t and $\%m_f$ is the final percentage mass. The obtained degrees of conversion for respective heating rates are shown in Fig. 4(a).

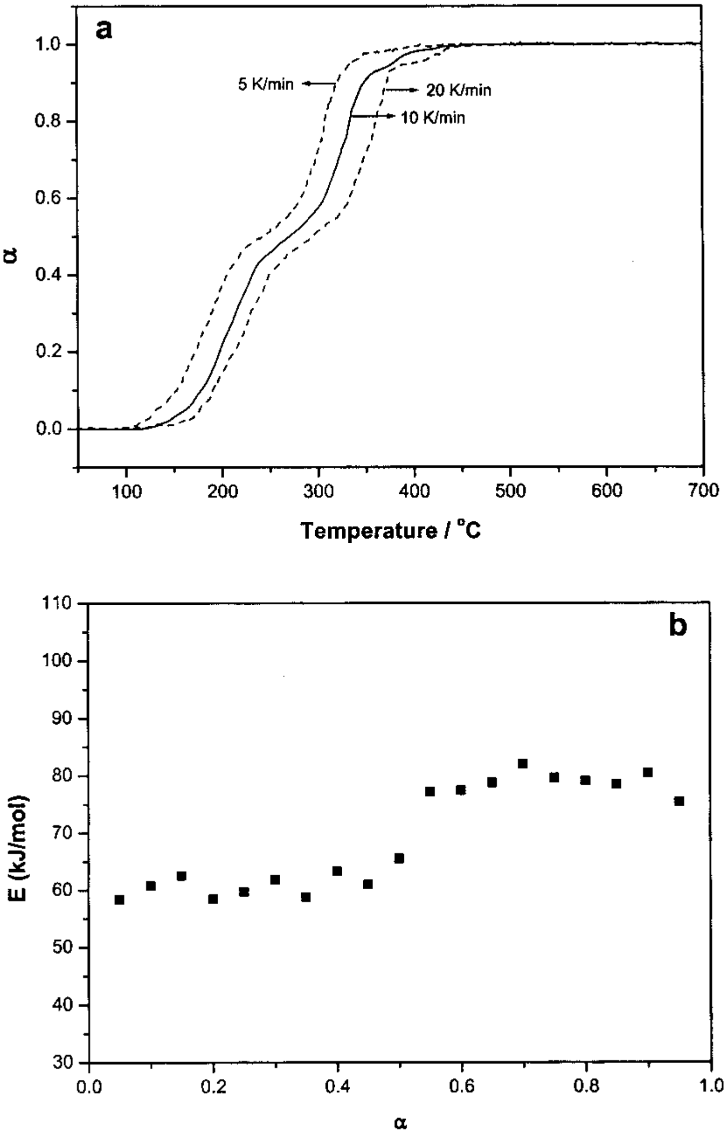

FIGURE 4 (a) Three experimental α–temperature dependences for decomposition of the complex $[Zn(benz)_2(3\text{-pymeth})_2]_n$ in air obtained at different heating rates (5, 10 and 20 K min^{-1}); (b) determined functional dependence of the activation energy, E_A, on the extent of conversion, α.

During evaluation, the integrated form of the kinetic equation under non-isothermal conditions [47] was expressed as in Eq. (2),

$$g(\alpha) = \frac{AE_A}{R\beta}\int_x^{\infty}\left(\frac{e^{-x}}{x^2}\right)\mathrm{d}x = \frac{AE_A}{R\beta}p(x) \tag{2}$$

where $x = E_A/RT$, A is the frequency factor, E_A is the activation energy, R is the molar gas constant, α is the fraction of the reacted material, T is the absolute temperature and $g(\alpha)$ is the functional form describing the kinetic model of the solid-state process.

For numerical evaluation of the temperature integral in Eq. (2), the Doyle approximation, Eq. (3), was used [48].

$$\log p(x) = -2.315 - 0.4567x \tag{3}$$

By combining Eqs. (2) and (3) the following expression, Eq. (4), is obtained

$$\log g(\alpha) = \log\left(\frac{AE_\mathrm{A}}{\beta R}\right) - 2.315 - \frac{0.4567E_\mathrm{A}}{RT} \tag{4}$$

For a number of experiments with different heating rates, β, we can write, for the same extent of reaction α, Eq. (5):

$$-\log\beta = \frac{0.4567E_\mathrm{A}}{RT} + \text{constant} \tag{5}$$

A plot of $\log\beta$ *versus* $1/T$ for a given value of α gives the activation energy E_A. Functional dependence of activation energy E_A on the extent of conversion α is shown in Fig. 4(b). The E_A dependence rises from about $60\,\mathrm{kJ\,mol^{-1}}$ in the conversion range $0.05 < \alpha < 0.45$ to near $80\,\mathrm{kJ\,mol^{-1}}$ for $0.55 < \alpha < 0.95$. The obtained dependencies indicate unambiguously a multi-step mechanism for decomposition of the complex. Moreover, functional dependence of activation energy on α increases and according to Vyazovkin [49] this means that parallel reactions take place during thermal decomposition.

Acknowledgments

This work was supported by the Grant Agency VEGA of the Slovak Ministry of Education (grant No. 1/9247/02). One of the authors (V.Z.) wishes to thank the Ministère délégué à la Recherche et aux Nouvelles Technologies of the French Republic for financial support during his stay at Madirel as part of the programme Accueil de jeunes chercheurs étrangers en séjour de recherche post-doctorale.

Supplementary Data

Crystallographic data have been submitted as supplementary material to the Cambridge Crystallographic Data Centre as supplementary material No. CCDC 212963. These data can be obtained free of charge via www.ccdc.cam.ac.uk/conts/retrieving.html (or from the CCDC, 12 Union Road, Cambridge CB2 1EZ, UK; Fax: +44 1223 336033; E-mail: deposit@ccdc.cam.ac.uk).

References

[1] B.L Vallee and D.S. Auld, *Biochem.* **24**, 5647 (1990).
[2] E. Kimura and T. Koike, *Adv. Inorg. Chem.* **44**, 229 (1997).

[3] W. Kaim and B. Schwederski, Bioinorganic Chemistry: Inorganic Elements in the Chemistry of Life (John Wiley & Sons, Chichester, 1994).
[4] C. Dendrinou-Samara, G. Tsotsou, L.V. Ekateriniadou, A.H. Kortsaris, C.P. Raptopoulou, A. Terzis, D.A. Kyriakidis and D.P. Kessissoglou, *J. Inorg. Biochem.* **71**, 171 (1998).
[5] B.D. Korant, J.C. Kauer and B.F. Butterworth, *Nature* **248**, 588 (1974).
[6] E. De Clerco, *Metal-Based Drugs* **4**, 173 (1997).
[7] B. Simó, L. Perelló, R. Ortiz, A. Castiñeiras, J. Latorre and E. Cantón, *J. Inorg. Biochem.* **81**, 275 (2000).
[8] O. Yamamoto, *Int. J. Inorg. Mat.* **3**, 643 (2001).
[9] Y.H. Cho, S.J. Lee, J.Y. Lee, S.W. Kim, C.B. Lee, W.Y. Lee and M.S. Yoon, *Int. J. Antimicrob. Agents* **19**, 576 (2002).
[10] S.C. Cunnane, Zinc: Clinical and Biochemical Significance (CRC Press, Boca Raton, FL, 1988).
[11] R.R. Warner, J.R. Schwartz, Y. Boissy and T.L. Dawson, *J. Am. Acad. Dermatol.* **45**, 897 (2001).
[12] C.L. Feucht, B.S. Allen and D.K. Chalker, *J. Am. Acad. Dermatol.* **3**, 483 (1980).
[13] E.J. van Hoogdalem, *J. Eur. Acad. Dermatol. Venereol.* **11**, S13 (1998).
[14] (a) K.B. Diehl, *Am. Fam. Physician* **54**, 1687 (1996); (b) D. Russell and A.D. Russell, *J. Infect.* **24**, 333 (1992).
[15] S.C. Rastogi, J.P. Lepoittevin, J.D. Johansen, P.J. Frosch, T. Menné, M. Bruze, B. Dreier, K.E. Andersen and I.R. White, *Contact Dermatitis* **39**, 293 (1998).
[16] E. Sainio and L. Kanerva, *Contact Dermatitis*, **33**, 100 (1995).
[17] M. Hanssen, E for Additives (Thorsons, HarperCollins Publishers, London, 1987).
[18] L.L. Dock, J.D. Floros and R.H. Linton, *J. Food Prot.* **63**, 1026 (2000).
[19] M. Islam, J. Chen, M.P. Doyle and M. Chinnan, *J. Food Prot.* **65**, 1411 (2002).
[20] European Union Directive 95/2/CE from 20.02.1995 on food additives, colourants and sweeteners, European Commission, Brussels.
[21] World Health Organisation, International Programme on Chemical Safety. *Benzoic Acid and Sodium Benzoate*, Concise International Chemical Assessment Document No. 26. Geneva, 2000.
[22] V. Zeleňák, M. Sabo, W. Massa and P. Llewellyn, *Inorg. Chim. Acta* (DOI: 10.1016/j.ica.2004.01.016).
[23] G.M. Sheldrick, SHELXS-97, Program for the Solution of Crystal Structures (University of Göttingen, Göttingen, Germany, 1997).
[24] G.M. Sheldrick, SHELXL-97, Program for the Refinement of Crystal Structures (University of Göttingen, Göttingen, Germany, 1997).
[25] K. Brandenburg (2000). DIAMOND 2.le, Crystal Impact GbR, Bonn.
[26] J. Moncol, M. Koman, M. Melnik and T. Glowiak, *Cryst. Eng. Comm.* **54**, 106 (2001).
[27] F. Valach, M. Tokarcik, P. Kubinec, M. Melnik and L. Macaskova, *Polyhedron* **16**, 1461 (1997).
[28] M. Melnik, K. Smolander and P. Sharrock, *Inorg. Chim. Acta* **103**, 187 (1985).
[29] H. Necefoglu, W. Clegg and A.J. Scott, *Acta Cryst.* **E57**, m462 (2001).
[30] H. Necefoglu, W. Clegg and A.J. Scott, *Acta Cryst.* **E57**, m465 (2001).
[31] P. Chaudhuri, C. Stockheim, K. Wieghardt, W. Deck, R. Gregorzik, H. Vahrenkamp, B. Nuber and J. We, *Inorg. Chem.* **31**, 1451 (1992).
[32] I. Potočňák. M. Dunaj-Jurčo and J. Černák, *Acta Cryst.* **C49**, 1496 (1993).
[33] J. Černák, I. Adzimová, F. Gerard and A.M. Hardy, *Acta Cryst.* **C51**, 392 (1995).
[34] K. Ogawa, K. Nakata and K. Ichikawa, *Bull. Chem. Soc. Jpn.* **70**, 2925 (1997).
[35] S. Uhlenbrock, R. Wegner and B. Krebs, *J. Chem. Soc., Dalton Trans.* 3731 (1996).
[36] S.S.S. Raj, H.K, Fun, P.S. Zhao, F.F Jian, D. Lu, X.J. Yang and X. Wang, *Acta Cryst.* **C56**, 742 (2000).
[37] M.R. Sundberg, *Acta Chem. Scand.* **48**, 195 (1994).
[38] W. Clegg, I.R. Little and B.P. Straughan, *Inorg. Chem.* **27**, 1916 (1988).
[39] D.H. Gibson, Y. Ding, R.L. Miller, B.A. Sleadd, M.S. Mashuta and J.F. Richardson, *Polyhedron* **18**, 1189 (1999).
[40] Y.Q. Lu, W.M. Lu, B. Wu and L.N. Wang, *J. Coord. Chem.* **53**, 15 (2001).
[41] ICDD Card No. 36-1451.
[42] S.C. Mojumdar, M. Melnik and E. Jona, *Thermochim. Acta* **352–353**, 127 (2000).
[43] T. Ozawa, *Bull. Chem. Soc. Jpn.* **38**, 1881 (1965).
[44] J.H. Flynn and L.A. Wall, *J. Res. Nat. Bur. Standards* **70A**, 487 (1966).
[45] M.E. Brown, M. Maciejewski, S. Vyazovkin, R. Nomen, J. Sempere, A. Burnham, J. Opfermann, R. Strey, H.L. Anderson, A. Kemmler, R. Keuleers, J. Janssens, H.O. Desseyn, C.R. Li, T.B. Tang, B. Roduit, J. Malek and T. Mitsuhashi, *Thermochim. Acta* **355**, 125 (2000).
[46] S. Vyazovkin, *Thermochim. Acta* **355**, 155 (2000).
[47] A.K. Galwey and M.E. Brown, In: M.E. Brown (Ed.), Handbook of Thermal Analysis and Colorimetry, Vol. I (Elsevier, Amsterdam, 1998), pp. 147–224.
[48] C.D. Doyle, *J. Appl. Polym. Sci.* **6**, 639 (1962).
[49] S.V. Vyazovkin and A.I. Lesnikovich, *Thermochim. Acta* **165**, 273 (1990).